Electronic Supplementary Material (ESI) for CrystEngComm.

Emissive Lanthanide Dicyanoaurate Coordination Polymers with 2,2′-Bipyridine Dioxide Antenna Groups and their Hydration States

Matthew L. Brown, Thomas E. Karpiuk, Daniel B. Leznoff *

Department of Chemistry, Simon Fraser University, 8888 University Drive, Burnaby, British Columbia, V5A 1S6, Canada. Email: dleznoff@sfu.ca

Supporting Information

Table S1 Ligand angles in the **1Ln** structures

Lanthanide	O-Ln-O (°)	Angle between aromatic rings (°)
Ce	69.56(7)	59.28
Nd	70.24(11)	58.30
Sm	70.61(5)	57.86
Eu	71.08(8)	58.23
Tb	71.4(2)	58.24
Dy	71.59(11)	57.61
Yb	72.34(6)	56.57

Table S2 Au···Au distances in the **1Ln** structures

Lanthanide	Au···Au Distance (Å)
Ce	3.2994(5)
Nd	3.3813(3)
Sm	3.3457(2)
Eu	3.29740(17)
Tb	3.3042(5)
Dy	3.2993(2)
Yb	3.30638(18)

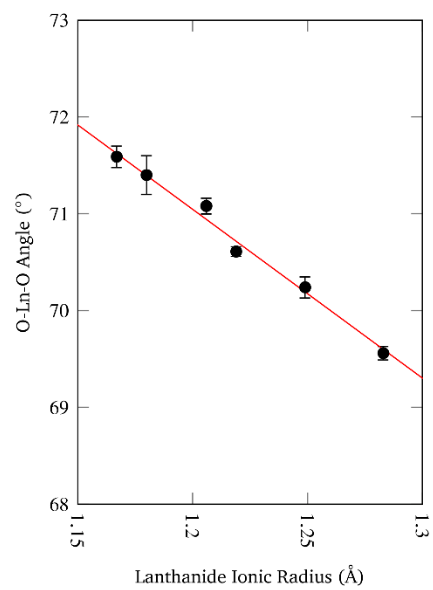

Fig. S1 The O-Ln-O bite angles in the **1Ln** structures plotted against the crystal radius (effective ionic radius + 0.14 Å) of the lanthanide ion with coordination number eight.[1] This data has been given an unweighted linear fit to $y = -17.44x + 91.975$ which gives an $R^2 = 0.9931$, indicating a strong linear correlation between lanthanide crystal radius and the O-Ln-O bond angle.

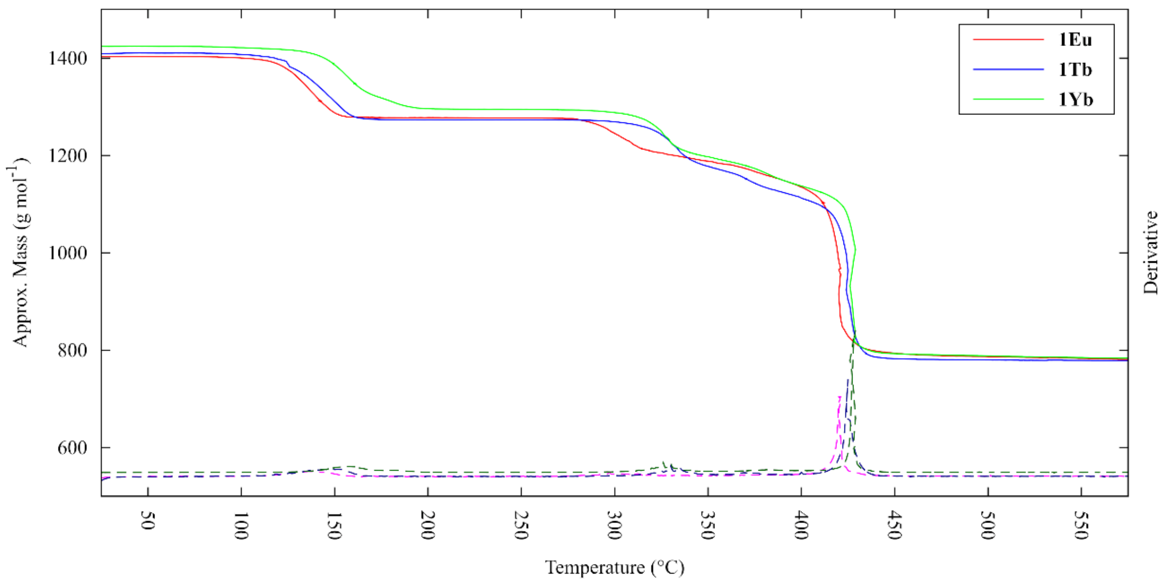

Fig. S2 Thermogravimetric analysis data samples of **1Ln**. Mass (solid lines) and the first derivative (dashed lines) plotted on separate axes.

Table S3 Yields of **1Ln**

Lanthanide	Reaction Scale (mmol)	Yield (mg)	Yield (%)	Evaporation Time (days)
La	0.40	16	23	54
Ce	0.05	27	27	64
Nd	0.05	33	47	16
Sm	0.05	32	46	17
Eu	0.05	23	33	31
Gd	0.05	49	70	16
Tb	0.05	51	72	16
Dy	0.05	44	62	31
Tm	0.05	49	69	16
Yb	0.05	48	67	61
Lu	0.05	48	67	17

Table S4 Elemental analysis results for **1Ln**

Ln		C (%)	H (%)	N (%)
Ce	Calc.	25.89	2.32	10.06
	Exp.	25.92	2.36	10.16
Nd	Calc.	25.81	2.31	10.04
	Exp.	25.97	2.69	10.20
Sm	Calc.	25.70	2.30	9.99
	Exp.	26.00	2.74	10.22
Eu	Calc.	25.67	2.30	9.98
	Exp.	25.76	2.32	10.05
Eu Desolv.	Calc.	24.49	1.26	10.98
	Exp.	24.38	1.55	10.93
Tb	Calc.	25.55	2.29	9.93
	Exp.	25.44	2.47	9.88
Dy	Calc.	25.48	2.28	9.91
	Exp.	25.57	2.51	10.05
Tm	Calc.	25.37	2.27	9.86
	Exp.	25.30	2.50	9.84
Yb	Calc.	25.29	2.26	9.83
	Exp.	25.30	2.62	9.80

Table S5 IR peaks for **1Ln**

Ln	Frequency (cm^{-1})
Ce	3729, 3417, 3091, 3190, 3125, 3106, 2972, 2888, *2180, 2164, 2145*, 1477, 1475, 1445, 1257, 1243, 1445, 1426, 1236, 1229, 1217, 1044, 1034, 850, 838, 776, 732, 718
Nd	3737, 3409, 3192, 3123, 3107, 3093, 2973, 2891, *2181, 2165, 2147*, 1477, 1475, 1446, 1426, 1423, 1258, 1244, 1237, 1230, 1217, 1045, 1033, 851, 838, 776, 733, 718
Eu	3416, 3199, 3126, 3110, 3093, 2974, 2888, *2182, 2165, 2147*, 1477, 1475, 1428, 1258, 1239, 1239, 1230, 1218, 1045, 851, 839, 776, 732, 719
Gd	3733, 3411, 3215, 3132, 3107, 3092, 2973, 2888, *2182, 2166, 2146*, 1477, 1475, 1427, 1257, 1245, 1239, 1231, 1219, 1045, 1033, 853, 839, 777, 733, 718
Tb	3735, 3414, 3206, 3125, 3108, 3093, 2973, 2886, 2443, 2355, *2183, 2166, 2146*, 1477, 1475, 1427, 1422, 1257, 1246, 1240, 1231, 1219, 1045, 1034, 856, 851, 840, 777, 733, 718
Dy	3735, 3410, 3215, 3121, 3109, 3093, 2974, 2889, *2183, 2166, 2147*, 1477, 1475, 1427, 1257, 1241, 1232, 1219, 1046, 851, 840, 777, 732, 718
Tm	3730, 3412, 3221, 3127, 3109, 3094, 2974, 2934, 2887, *2184, 2166, 2147*, 1477, 1457, 1449, 1446, 1427, 1422, 1258, 1248, 1242, 1232, 1221, 1046, 1034, 857, 852, 841, 776, 733, 718
Yb	3410, 3214, 3128, 3109, 3095, 2974, 2891, *2185, 2166, 2147*, 1477, 1475, 1426, 1259, 1242, 1233, 1221, 1046, 841, 776, 718
25:75 SmTb	3737, 3412, 3205, 3127, 3109, 3093, 2973, 2886, *2182, 2166, 2147*, 1477, 1475, 1427, 1257, 1246, 1239, 1231, 1219, 1045, 850, 839, 777, 732, 718
75:25 SmTb	3664, 3412, 3205, 3127, 3109, 3093, 2973, 2892, *2182, 2166, 2147*, 1477, 1475, 1427, 1257, 1246, 1239, 1231, 1219, 1045, 850, 839, 777, 732, 718
50:50 CeSm	3409, 3207, 3111, 3094, 2973, 2889, *2181, 2165, 2155, 2146*, 1477, 1475, 1446, 1426, 1423, 1257, 1245, 1237, 1230, 1218, 1045, 1032, 850, 838, 775, 732, 718

*ν*CN peaks are *marked*.

Table S6 Raman peaks for **1Ln**

Ln	Laser (nm)	Frequency (cm^{-1})
Ce	514	3091, 3078, *2180, 2162*, 1619, 1608, 1569, 1507, 1423, 1313, 1256, 1244, 1218, 1162, 1122, 1105, 1074, 1053, 1001, 960, 885, 856, 787, 748, 734, 639, 589, 557, 537, 484, 410, 351, 307, 287, 279, 174, 130
Eu	785	3080, 3030, 2921, *2182, 2161*, 1619, 1605, 1571, 1315, 1258, 1246, 1220, 1156, 1123, 1054, 1034, 885, 856, 839, 748, 735, 715, 713, 639, 587, 558, 526, 486, 472, 303, 291, 289, 181, 151, 149, 141
Tb	785	3079, 3033, 2922, *2183, 2167, 2161*, 1620, 1606, 1574, 1509, 1315, 1257, 1248, 1221, 1157, 1124, 1053, 1034, 885, 856, 840, 749, 735, 639, 584, 558, 527, 488, 447, 320, 305, 290, 283, 189, 150, 143, 118
Dy	785	3080, 3031, 2919, 2886, *2183, 2161*, 1619, 1606, 1573, 1508, 1444, 1424, 1315, 1258, 1248, 1221, 1156, 1123, 1051, 1034, 886, 857, 840, 749, 735, 713, 639, 588, 557, 527, 517, 488, 448, 360, 307, 290, 283, 186, 152, 143, 114
Yb	785	3080, 3030, 2920, 2874, 2871, 2777, 2631, 2492, 2338, 2249, *2185, 2162*, 1619, 1606, 1574, 1509, 1477, 1444, 1315, 1272, 1259, 1250, 1220, 1158, 1123, 1059, 1051, 1036, 1001, 956, 886, 876, 858, 843, 786, 750, 736, 640, 587, 558, 530, 519, 490, 448, 419, 364, 322, 311, 291, 286, 198, 178, 154, 145, 121

νCN peaks are *marked*.

Table S7 Yields of **2Ln**

Lanthanide	Reaction Scale (mmol)	Yield (mg)	Yield (%)	Evaporation Time (days)
La	0.05	43	62	3
Ce	0.05	1	13	48
Nd	0.05	19	27	48
Sm	0.05	23	33	17
Eu	0.05	45	64	17
Tb	0.05	25	35	17
Tm	0.05	24	34	48
Yb	0.05	55	77	17

Table S8 Elemental analysis results for **2Ln** · 5 H_2O

Ln		C (%)	H (%)	N (%)
Ce	Calc.*	22.47	2.18	10.08
	Exp.	22.25	2.34	9.84
Eu	Calc.	22.87	1.92	10.26
	Exp.	23.28	1.73	10.69
Gd	Calc.	22.78	1.91	10.22
	Exp.	22.47	2.23	10.20
Tb	Calc.	22.75	1.91	10.21
	Exp.	22.87	2.16	10.20
Dy	Calc.	22.70	1.90	10.18
	Exp.	23.17	2.18	10.42
Tm	Calc.	22.59	1.90	10.13
	Exp.	22.99	2.01	10.23
Yb	Calc.	22.52	1.89	10.10
	Exp.	22.60	2.29	10.22

*Calc. amounts based on **2Ce** · 6 H_2O due to better match; sample may not have fully transformed to **2Ce** · 5 H_2O before being analyzed.

Table S9 IR peaks of **2Ln** · 6 H_2O

Ln	Frequency (cm^{-1})
Eu	3635, 3632, 3625, *2177, 2157*, 1475, 1425, 1422, 1257, 1248, 1236, 1228, 1216, 848, 837, 777, 775
Tb	3632, 3308, 3140, *2178, 2172, 2157, 2147*, 1477, 1475, 1426, 1423, 1258, 1249, 1236, 1229, 1216, 850, 839, 775

*ν*CN peaks are *marked*.

Table S10 IR peaks of **2Ln** · 5 H_2O

Ln	Frequency (cm^{-1})
Nd	3741, 3388, 3131, 3096, 3064, *2179, 2148*, 1642, 1478, 1475, 1425, 1423, 1257, 1232, 1224, 1215, 847, 836, 768
Sm	3631, 3303, 3137, 3079, 2175, *2171, 2155, 2141*, 1477, 1475, 1426, 1423, 1260, 1249, 1236, 1228, 1216, 851, 837, 780, 774
Eu	3635, 3632, 3625, 3310, 3217, *2175, 2171, 2155*, 1475, 1425, 1422, 1259, 1249, 1236, 1228, 1216, 848, 837, 780, 774
Gd	3740, 3631, 3315, 3229, 3143, 3079, *2176, 2171, 2155*, 1477, 1475, 1426, 1426, 1260, 1249, 1236, 1228, 1217, 850, 839, 774, 734, 714
Tb	3636, 3632, 3625, 3310, 3217, *2177, 2172, 2156*, 1475, 1425, 1422, 1260, 1249, 1236, 1228, 1216, 849, 838, 774
Tm	3636, 3330, 3144, 3094, *2180, 2176, 2157, 2146*, 1477, 1475, 1426, 1422, 1259, 1249, 1237, 1229, 1217, 850, 840, 776
Yb	3636, 3330, 3144, 3094, *2181, 2176, 2157, 2146*, 1477, 1475, 1426, 1422, 1259, 1249, 1237, 1229, 1217, 850, 840, 776

*ν*CN peaks are *marked*.

Table S11 IR peaks of **2Ln** · 4 H_2O

Ln	Frequency (cm^{-1})
Sm	3636, 3635, 3624, 3310, 3217, *2174, 2170, 2154*, 1475, 1425, 1422, 1259, 1249, 1237, 1228, 1217, 851, 839, 774
Eu	3635, 3632, 3625, 3310, 3217, *2170, 2154*, 1475, 1425, 1422, 1259, 1249, 1237, 1228, 1218, 848, 839, 774
Tb	3310, 3217, *2171, 2154*, 1475, 1425, 1422, 1259, 1250, 1237, 1228, 1218, 849, 839, 774
Dy	3741, 3327, 3229, 3143, 3101, 3088, 3079, *2187, 2171, 2154*, 1477, 1475, 1425, 1423, 1260, 1250, 1236, 1228, 1218, 849, 840, 774

*ν*CN peaks are *marked*.

Table S12 IR peaks of **2Ln** · 0 H_2O

Ln	Frequency (cm^{-1})
Sm	3338, 3125, 3108, 3085, 3064, *2164, 2146, 2138*, 1477, 1475, 1427, 1261, 1247, 1239, 1217, 850, 838, 781, 768, 717
Eu	3338, 3125, 3108, 3085, 3064, *2165, 2146, 2138*, 1477, 1475, 1427, 1261, 1247, 1239, 1218, 850, 838, 781, 768, 717
Dy	3338, 3125, 3108, 3085, 3064, *2167, 2146, 2138*, 1477, 1475, 1427, 1261, 1248, 1240, 1218, 852, 839, 782, 768, 717

*ν*CN peaks are *marked*.

Table S13 Raman peaks of **2Ln** · 5 H_2O

Ln	Laser (nm)	Frequency (cm^{-1})
La	785	3086, *2169*, 1620, 1604, 1572, 1509, 1317, 1256, 1160, 1069, 1035, 877, 858, 733, 639, 586, 556, 534, 481, 300, 290, 182, 143
Nd	514	3096, 3081, 3037, *2197, 2154*, 1620, 1605, 1570, 1507, 1317, 1259, 1219, 1155, 1055, 886, 858, 734, 639, 589, 557, 488, 407, 300, 281, 139, 121
Sm	514	3197, 3136, 3086, 3081, 3037, 2923, 2783, 2702, 2626, 2460, *2176, 2156*, 1621, 1605, 1571, 1508, 1317, 1259, 1250, 1240, 1217, 1155, 1103, 1069, 1055, 1034, 887, 859, 790, 750, 734, 639, 589, 557, 536, 525, 525, 491, 412, 404, 310, 300, 281, 178, 148, 137, 121
Gd	785	3078, *2174, 2156*, 1619, 1606, 1569, 1507, 1424, 1317, 1260, 1219, 1162, 1154, 1102, 1070, 1054, 1033, 886, 858, 788, 734, 639, 587, 557, 535, 526, 489, 411, 403, 366, 300, 283, 176, 149, 138
Tb	514	3132, 3097, 3080, *2174, 2163*, 1621, 1605, 1571, 1507, 1476, 1426, 1315, 1259, 1249, 1220, 1154, 1117, 1054, 1034, 858, 790, 735, 638, 588, 557, 527, 491, 448, 411, 364, 316, 300, 283, 178, 148, 109

*ν*CN peaks are *marked*.

Table S14 Elemental analysis results for 50:50 SmTb blends

Series		C (%)	H (%)	N (%)
1Ln	Calc.	25.62	2.29	9.96
	Exp.	25.81	3.00	10.17
2Ln · 5 H_2O	Calc.	22.83	1.92	10.24
	Exp.	22.36	1.89	9.76

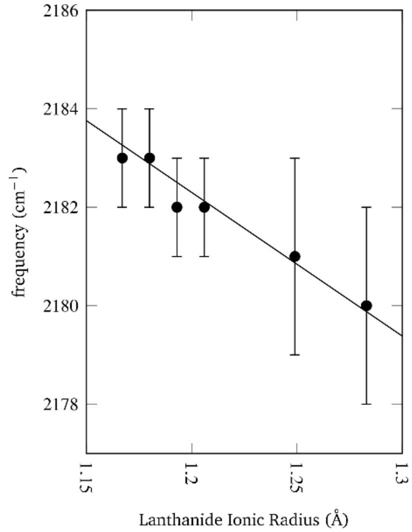

Fig. S3 Frequency of the *ν*CN stretching mode plotted versus lanthanide ionic radius for **1Ln** compounds.[1]

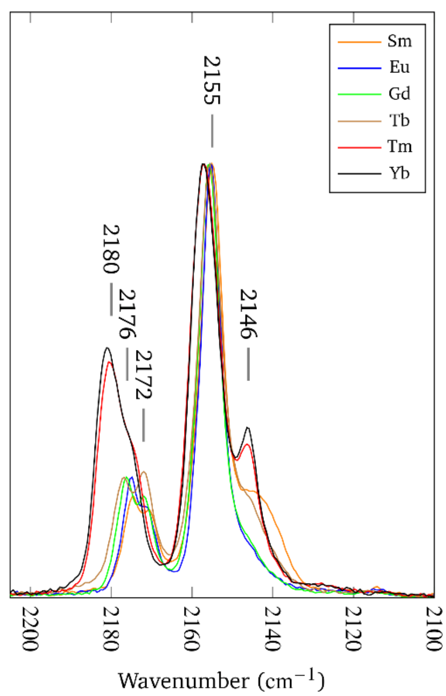

Fig. S4 *ν*CN region of the **1Ln** IR spectra.

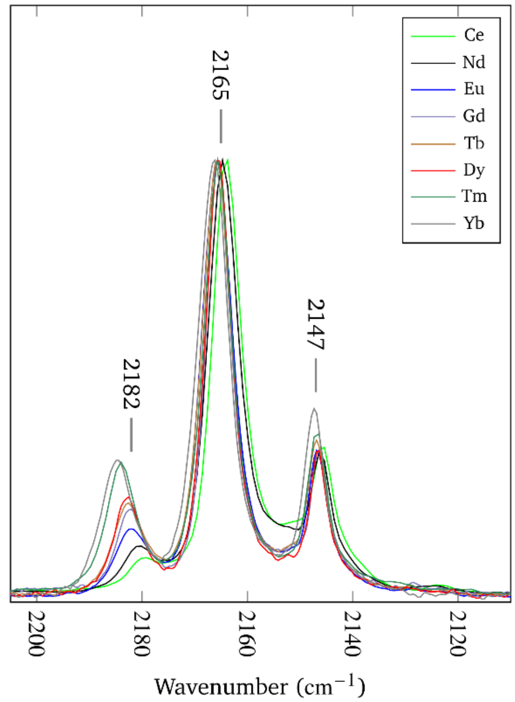

Fig. S5 νCN region of the **2Ln** · 5 H_2O IR spectra.

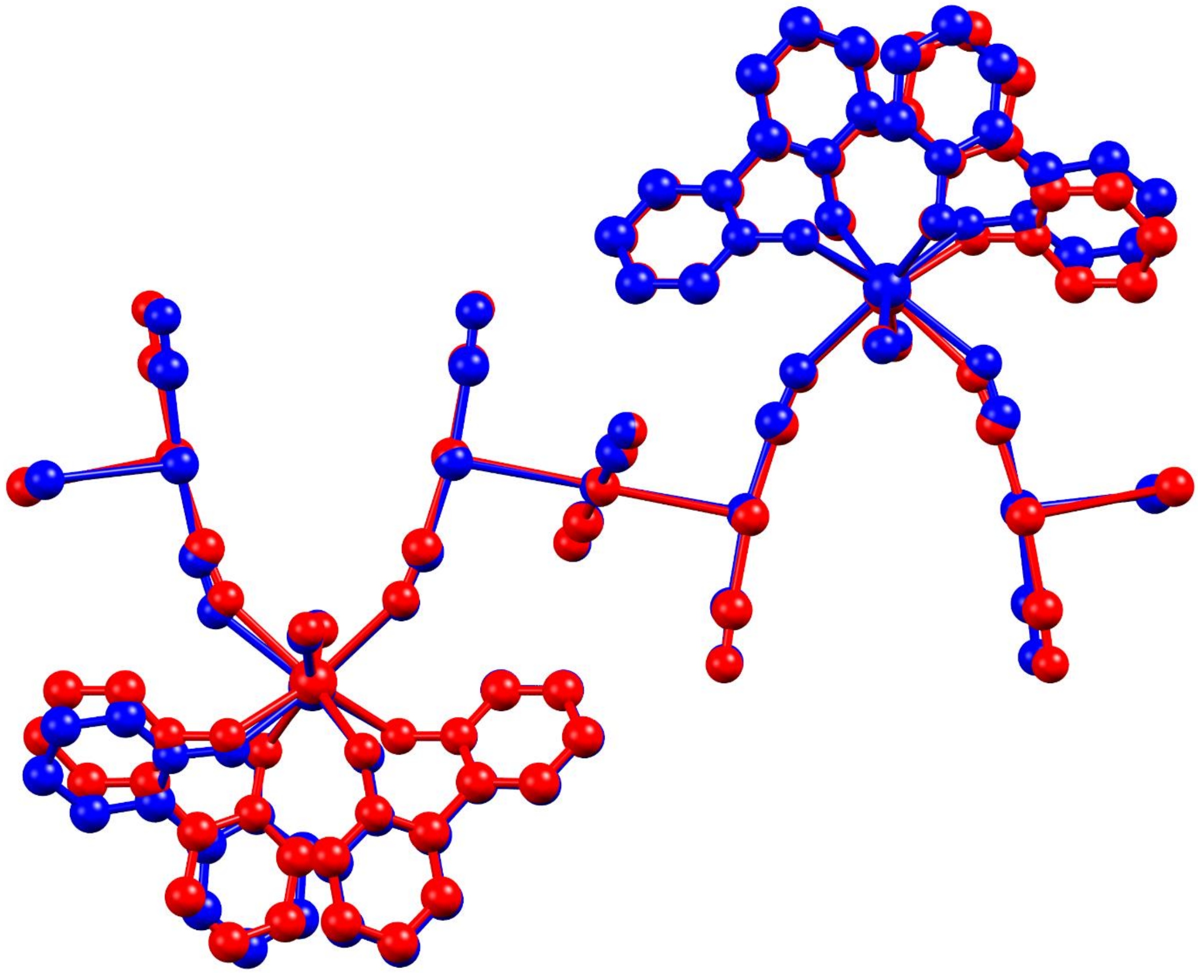

Fig. S6 Overlay of the structures of **2Ln** · 6 H_2O (Red) and **2Ln** · 5 H_2O (Blue) showing that loss of t he water molecule causes minimal long-range changes in the structure.

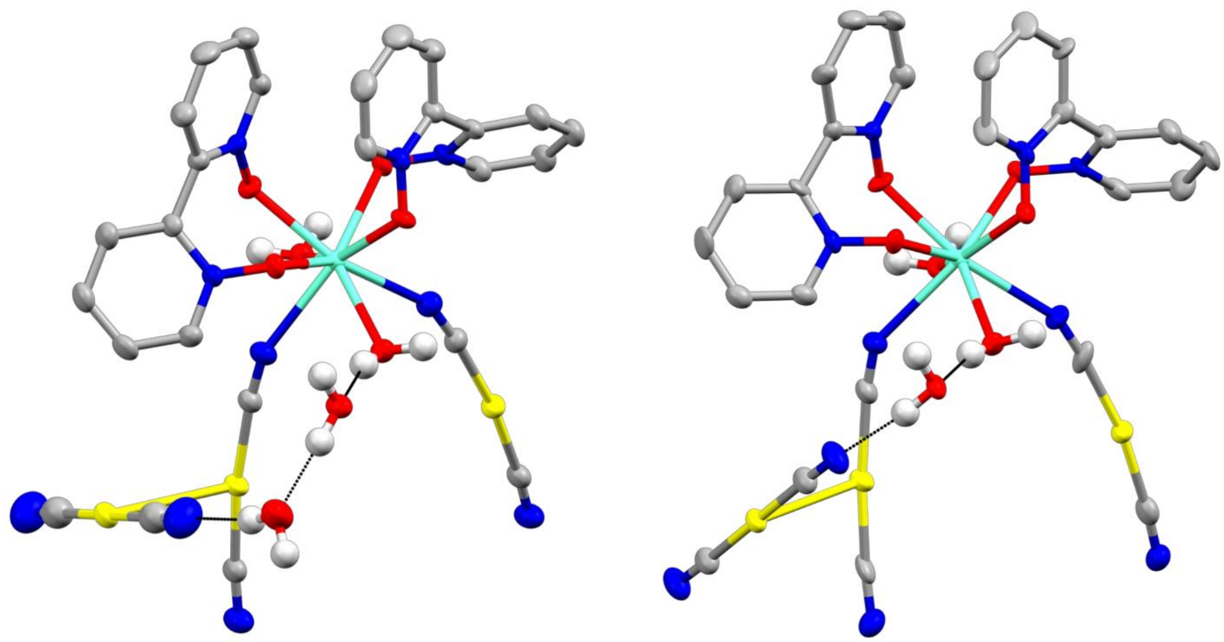

Fig. S7 Comparison between the hydrogen bonding networks of **2Ln** · 6 H_2O (Left) and **2Ln** · 5 H_2O (Right). The terminal cyanide shifts to restore the hydrogen bond with the remaining water molecule after water loss occurs.

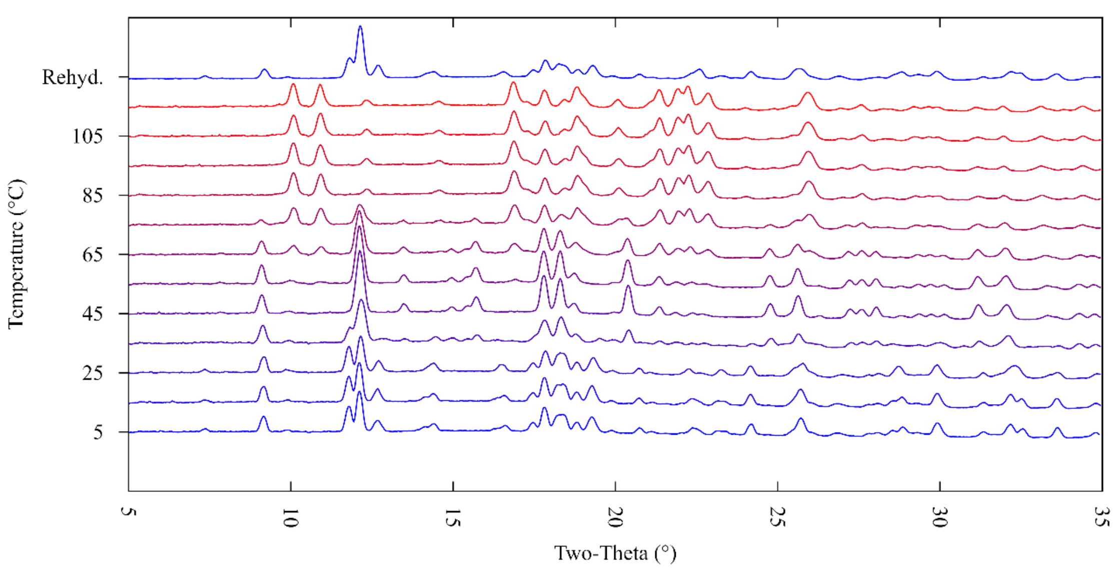

Fig. S8 Variable temperature powder X-Ray diffractograms of **2Yb** showing successive dehydration events. The top diffractogram illustrates that the dehydration is reversible. Rehydration was accomplished by introducing the dehydrated sample to water vapor.

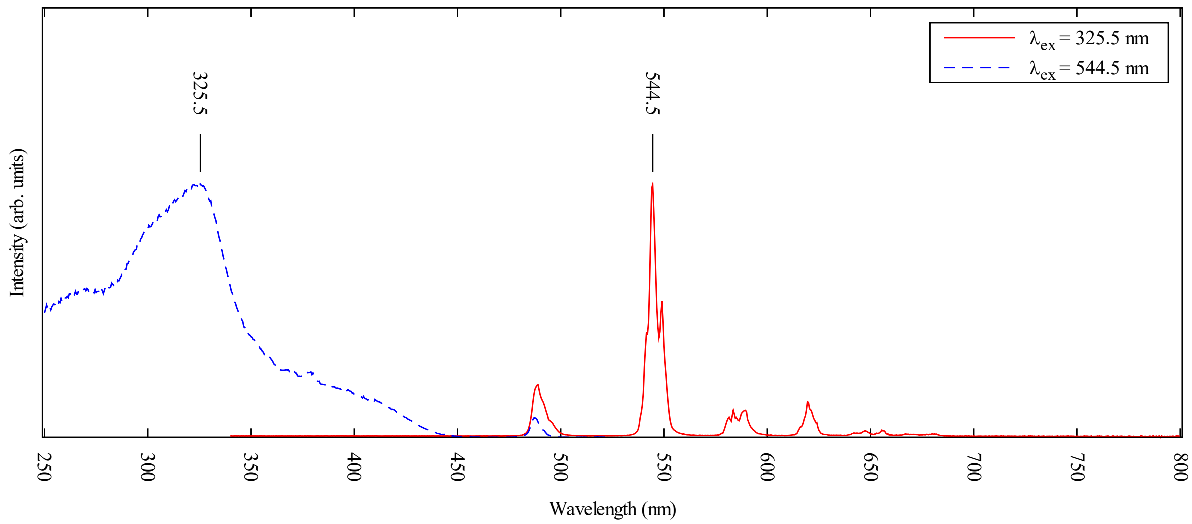

Fig. S9 Solid state luminescence spectra of **1Tb**. The compound was emitting bright green light, as shown in Figure 10.

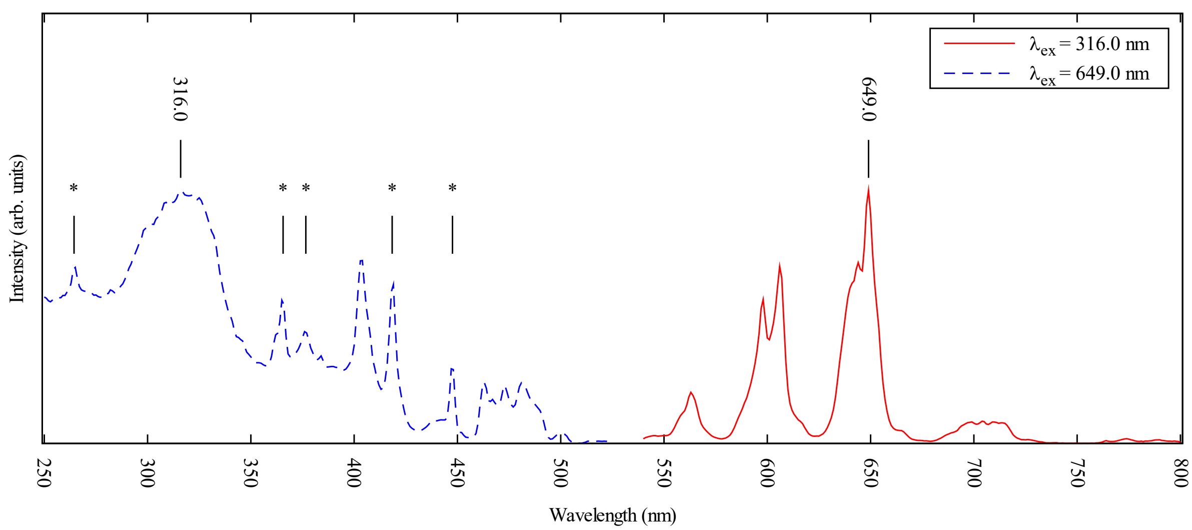

Fig. S10 Solid state luminescence spectra of **1Sm** taken on a powdered sample that was emitting red light. * denotes a peak due to an instrumental artifact.

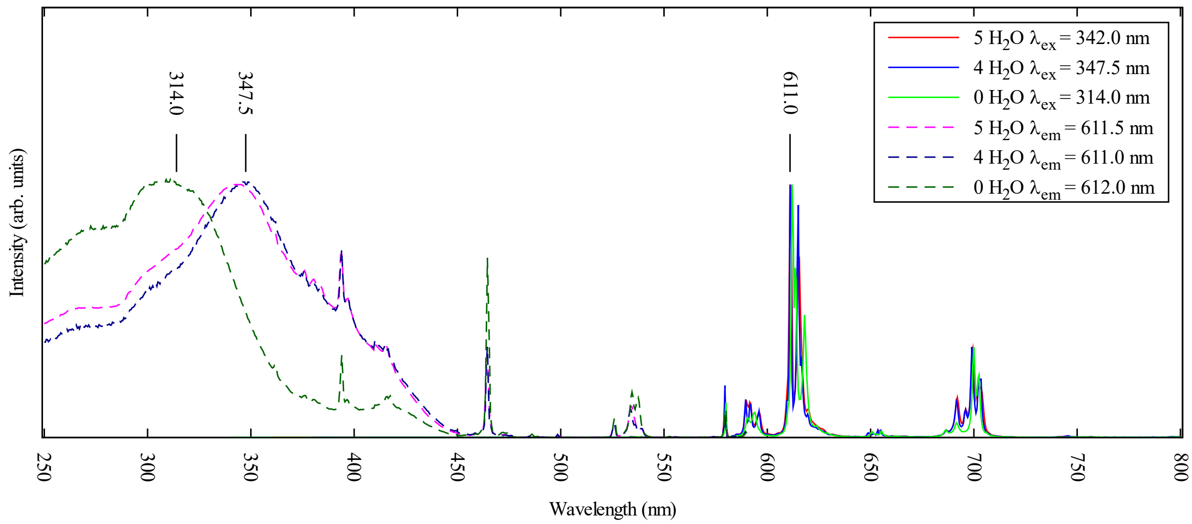

Fig. S11 Solid state luminescence spectra of **2Eu** · 5 H_2O, **2Eu** · 4 H_2O, and **2Eu** · 0 H_2O demonstrating its bright red emission. All data in this series were acquired on the same sample after successive dehydrations. Not all emission and excitation wavelengths are marked on the figure since they are extremely close to one another.

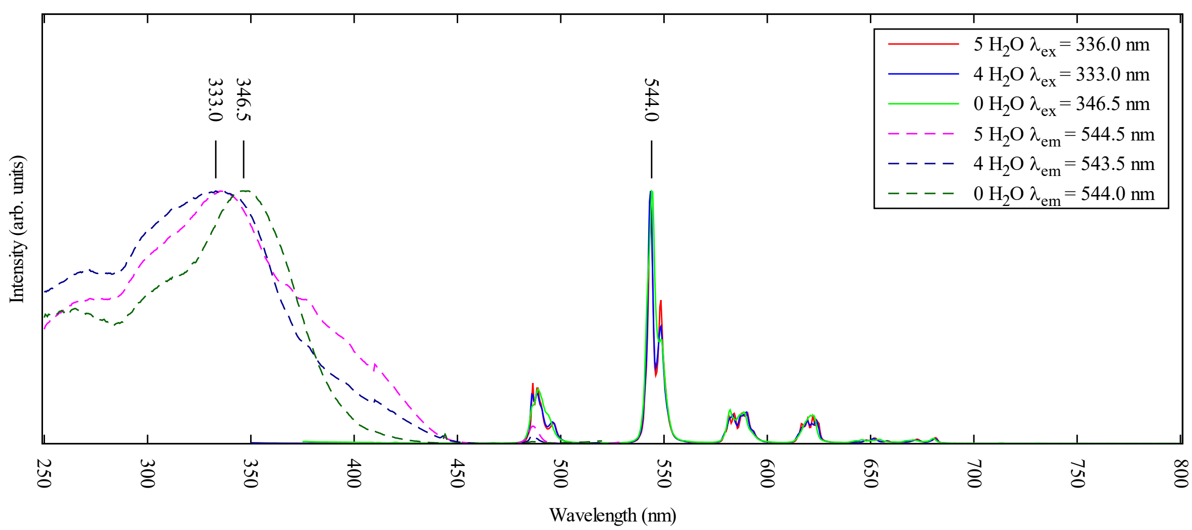

Fig. S12 Solid state luminescence spectra of **2Tb** · 5 H_2O, **2Tb** · 4 H_2O, and **2Tb** · 0 H_2O demonstrating its bright green emission. Not all emission and excitation wavelengths are marked on the figure since they are extremely close to one another.

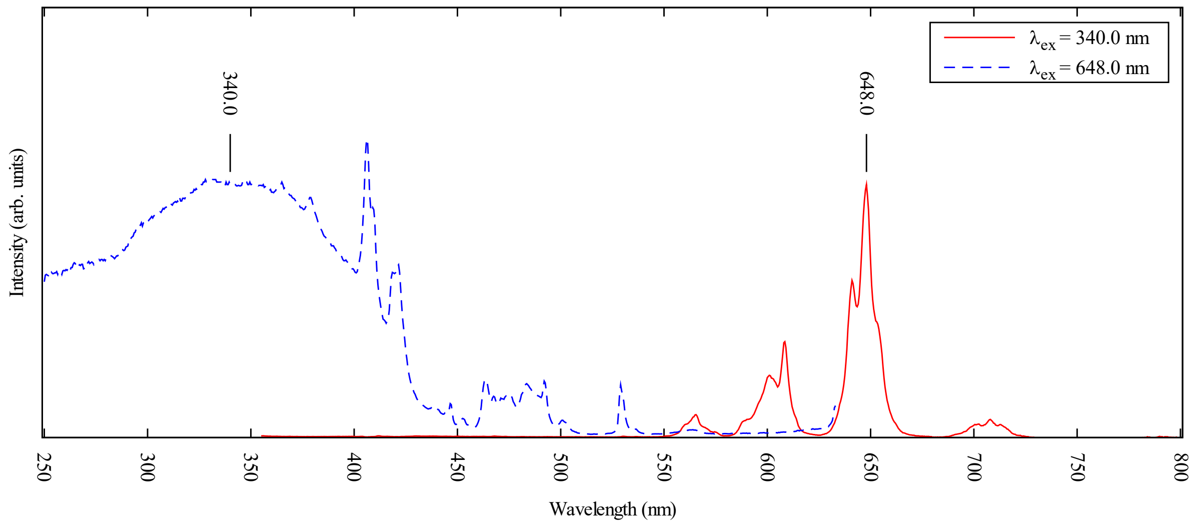

Fig. S13 Solid state luminescence spectra of **2Sm** · 5 H_2O, demonstrating its faint red emission.

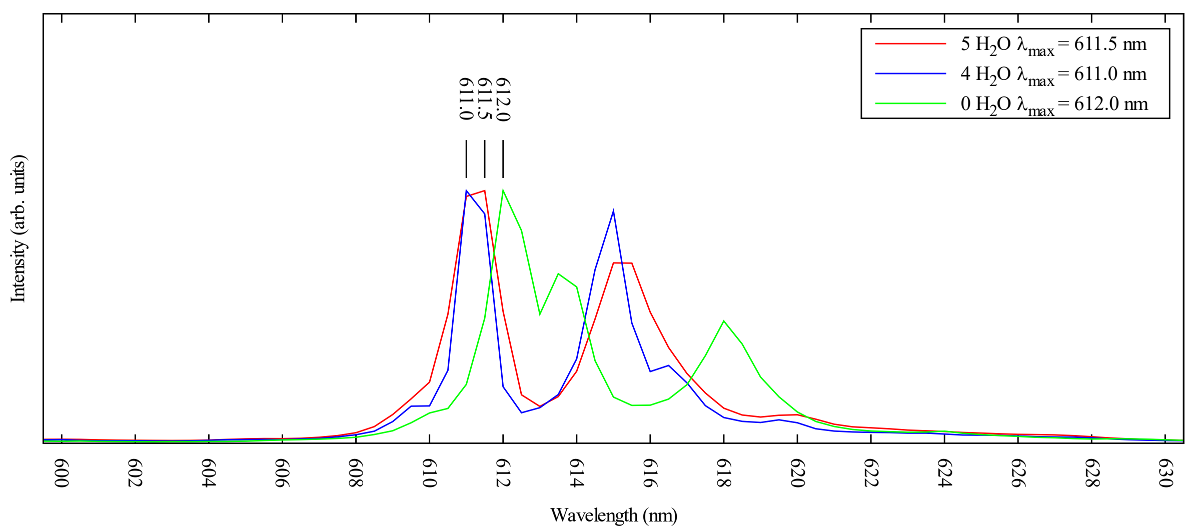

Fig. S14 Solid state luminescence spectra of **2Eu** · 5 H_2O, **2Eu** · 4 H_2O, and **2Eu** · 0 H_2O showing the changes in the approx. 612 nm $^5D_0 \rightarrow {}^7F_2$ hypersensitive transition peak in response to desolvation. All data in this series were acquired on the same sample after successive dehydration events.

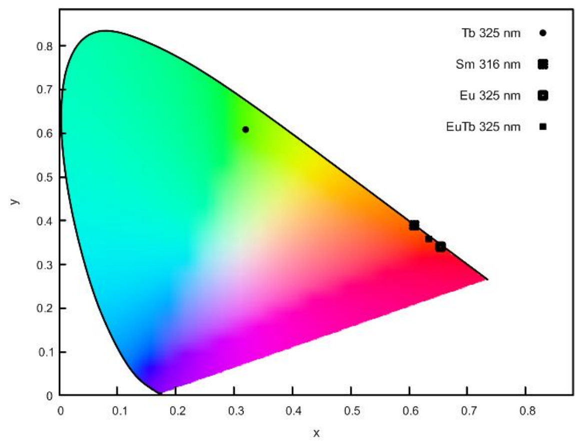

Fig. S15 CIE 1931 diagram showing the colours of various species of **1Ln**.

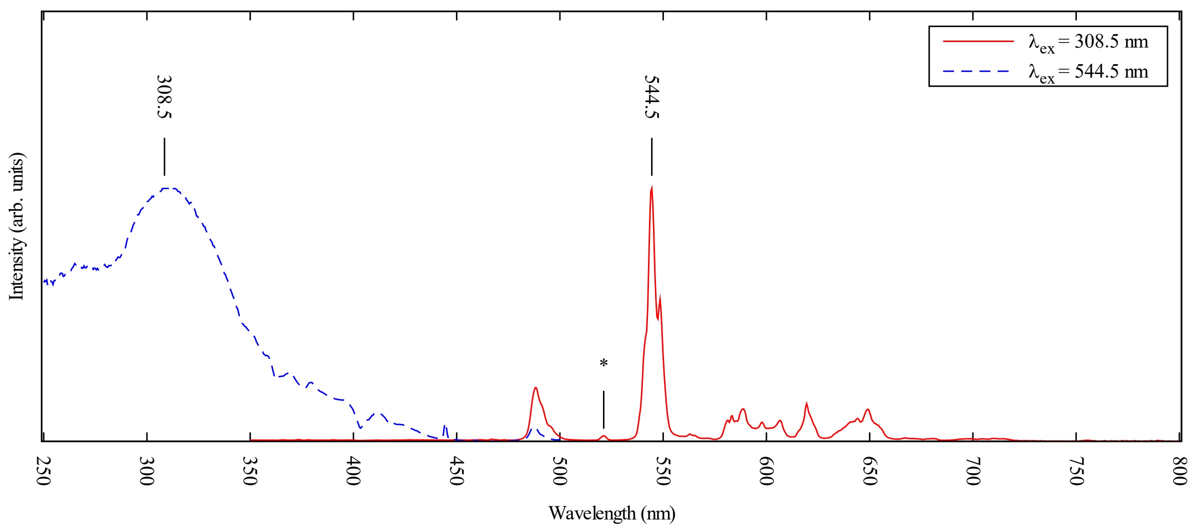

Fig. S16 Solid state luminescence spectra of 50:50 **1SmTb** showing that excitation into the ligand manifold produces both Tb- and Sm-based emission. * denotes a peak due to an instrument artifact.

References

(1) R. D. Shannon, *Acta Crystallogr. A* **1976**, *32*, 751–767.